Alpha-particle emission from the reaction 1354 MeV ^{165}Ho + ^{181}Ta

L. G. Sobotka, R. J. McDonald, G. J. Wozniak, D. J. Morrissey,* A. J. Pacheco,† and L. G. Moretto
Nuclear Science Division, Lawrence Berkeley Laboratory, University of California, Berkeley, California 94720
(Received 1 February 1983)

The emission of α particles from the deep-inelastic reaction 1354 MeV ^{165}Ho + ^{181}Ta has been studied. Alpha particles were detected in coincidence with a projectilelike fragment, both in and out of the reaction plane. Average velocity diagrams, α-particle energy spectra as a function of angle, and α-particle angular distributions are presented. The in-plane data show that the bulk of the α particles in coincidence with the deep-inelastic exit channel can be explained by evaporation from the fully accelerated fragments. The out-of-plane α-particle angular distribution data together with gamma-ray multiplicity data from previous work give a consistent picture of the transfer and partitioning of angular momentum between the two fragments.

[NUCLEAR REACTIONS ^{181}Ta(^{165}Ho, HIα)E_{lab}=1354 MeV: measured $\sigma_\alpha(E_\alpha,\theta_\alpha,\phi_\alpha)$, in- and out-of-plane anisotropies; deduced α-particle multiplicity, nuclear temperature.]

I. INTRODUCTION

Compound nuclei deexcite predominantly by the evaporation of light particles (LP's). The energy spectra and angular distributions of these LP's contain information on the temperature (T) and spin (I) of the emitting nucleus. By studying the sequential LP decay from the fragments produced in deep-inelastic (DI) reactions, insight regarding the thermal properties and the angular momentum degrees of freedom associated with these reactions can be obtained.

Two excellent examples of the use of LP's for these purposes are the studies of Eyal *et al.*[1] and Babinet *et al.*[2] In the former study, neutron emission from the reaction ^{166}Er + ^{86}Kr at 7.0 MeV/nucleon was measured for the DI component of the reaction. This study concluded that the equilibration of the excitation energy between the two exit channel nuclei occurs during the lifetime of the intermediate complex. This conclusion is supported by two experimental observations. The first of these is that the mean number of evaporated particles from the two reaction products indicates that the partition of the total dissipated energy between the two fragments is in proportion to their masses. (Such a partition is required by the thermal equilibrium conditions.[3]) Detailed studies of neutron emission from the systems ^{165}Ho + ^{56}Fe at 8.5 MeV/nucleon[4] and ^{197}Au + ^{63}Cu at 5.8 MeV/nucleon[5] have reached the same conclusion. The second experimental observation is that the temperatures of the two fragments (deduced from the neutron energy spectra) are the same, within the experimental uncertainties.

In the second example,[2] in- and out-of-plane α-particle angular distributions were measured for the DI component of the reaction ^{58}Ni + ^{40}Ar at 7.0 MeV/nucleon. The kinematics of this system allows the out-of-plane α-particle emission from the targetlike nucleus to be isolated by careful selection of the angle of the heavy ion detector as well as of the in-plane angle for the out-of-plane α-particle detectors. Individual fragment spins were extracted from the out-of-plane distributions as a function of mass asymmetry. The trend of these spins with mass asymmetry agreed with the rigid rotation predictions. This result was in agreement with earlier γ-ray multiplicity (M_γ) work[6,7] on similar systems, which also suggests that rigid rotation was achieved during the lifetime of the DI complex. More recently, this conclusion has also been shown to be valid for the heavier system ^{nat}Ag + ^{84}Kr at 7.9 MeV/nucleon.[8] The verification of rigid rotation for this near symmetric system is quite significant because M_γ studies, which provide information on the sum of the two fragment spins, were unable to provide evidence that allows for a clear distinction between the rotation limits of rolling and sticking.

The studies mentioned above rely on the identification of the source of the LP's. Most studies have concluded that the fully accelerated fragments are the dominant sources of the LP's. This result is in agreement with statistical model calculations that predict that LP evaporation times are longer than the heavy-ion interaction time.[4] However, recent data on ^{40}Ar and ^{56}Fe induced reactions[9–11] indicate that LP evaporation before scission of the intermediate complex can be substantial under certain conditions. The prescission LP emission process presents the tantalizing possibility of studying the intermediate complex during its very short lifetime.

In this paper we report on the results of a study of α-particle emission from the ^{181}Ta + ^{165}Ho reaction at 8.2 MeV/nucleon. The values of several relevant reaction parameters are listed in Table I. The light particle emission from this system is interesting for several reasons. First, this system is heavier and has more angular momentum than any of the systems previously studied by LP techniques. Furthermore, the reaction is dominated by a single process (DI), which simplifies the theoretical interpretation. Because of these qualities the Ho + Ta system has the potential for providing important information on the conditions needed for prescission emission. The data relevant to the question of the emission source(s) are

TABLE I. Parameters of the reaction $^{181}_{73}$Ta + $^{165}_{67}$Ho at 1354 MeV. [These values were calculated assuming spherical fragments where the distance between fragment centers is given by $1.225\,(A_L^{1/3}+A_H^{1/3})+2$ fm.]

c.m. energy	708. MeV
Coulomb energy	450. MeV
$E_{\text{c.m.}}/B_{\text{Coul}}$	1.6
Lab grazing angles (θ_{gr})	
projectile	29°
target	62°
$l_{\max}$	$513\hbar$
l_{rms}	$362\hbar$
Mass asymmetry	0.52
Moment of inertia ratio $\frac{\mathscr{I}_H}{\mathscr{I}_L+\mathscr{I}_H}$	0.54

presented in Sec. IV, some of which have been published previously.[12] In Sec. V the out-of-plane α-particle data from the ^{165}Ho + ^{181}Ta system are used to confirm results concerning the angular momentum degrees of freedom obtained from previous M_γ and γ-ray anisotropy work.[13]

II. EXPERIMENTAL TECHNIQUES

A natural Ta target (1.4 mg/cm^2) was bombarded with 8.2 MeV/nucleon ^{165}Ho ($\sim$10 nA) from the Lawrence Berkeley Laboratory SuperHILAC. A solid state detector (300 μm) positioned at the classical grazing angle (29°) was used to detect the projectilelike fragment and to define the reaction plane. On the opposite side of the beam, five solid state ΔE-E telescopes (40 μm, 5 mm) were used to detect the α particles. This detection apparatus is described in detail in Ref. 8. The only significant difference is that a single detector rather than a telescope was used to detect the projectilelike fragment. Therefore, neither the charge nor the mass of this fragment was determined in this experiment.

The beam energy was measured at regular time intervals during the experiment. These measurements were made either with a calibrated solid-state detector, applying a pulse height defect correction,[14] or by use of a phase probe, which measures the beam velocity. The mean interaction energy calculated at the center of the target was 1354 MeV. All α-particle telescopes and their associated electronics were calibrated with a pulser, which had been absolutely calibrated with a ^{212}Pb α-particle source. The heavy-ion (HI) detector was calibrated by elastic scattering at four bombarding energies on a thin (0.53 mg/cm^2) ^{197}Au target.

The absolute efficiencies of the α-particle telescopes were measured with a ^{241}Am source of known activity and the relative efficiencies were checked with a ^{212}Pb source. The measured solid angles agreed to within $\pm$3% of the geometric solid angle. Tantalum absorbers of approximately 9 mg/cm^2 were placed in front of the LP telescopes to reduce the rates of heavy ions, x rays, and low-energy electrons striking these counters. The absorber thicknesses were determined by α-particle energy loss measurements. These thicknesses along with the solid angles for all angles at which coincidence data were acquired are presented in Table II. The detection threshold for α particles was approximately 10 MeV, primarily due to the thickness of the first element of the telescope rather than the absorbers.

III. DATA ANALYSIS

It was assumed that the primary mass of the detected fragment (before particle evaporation) was that of the projectile (165 u) and that the primary mass of the undetected fragment was that of the target (181 u). This assumption is motivated by several considerations. The first of these is the bias towards detecting the projectilelike fragment when a HI is detected at the projectile grazing angle (29°). This bias can be understood by examining the Wilczynski plots for the similar systems ^{208}Pb + ^{110}Pd (Ref. 15) and ^{136}Xe + ^{207}Bi (Ref. 16). These plots not only show that the deflection function does not exhibit negative angle scattering, but also that the cross section, independent of energy loss, is focused into an angular region near the classical grazing angle when the bombarding energy is high enough so the reactions are not dominated by Coulomb effects. This suggests that, for the ^{165}Ho + ^{181}Ta system at 1354 MeV ($E_{\text{c.m.}}/B_{\text{Coul}}=1.6$, which is the same ratio as for the ^{136}Xe + ^{207}Bi study), the projectilelike and targetlike fragments will be focused into angular regions close to their respective laboratory grazing angles. Since the grazing angle of the target in the laboratory system is more than 30° behind that of the projectile, a strong selection on projectilelike fragments should be provided by placing the HI detector at the projectile grazing angle.

A second reason for using the entrance channel masses as the primary exit channel masses is that for both of the

TABLE II. ^{181}Ta + ^{165}Ho (1354 MeV) coincidence data.

Angle ϕ_L/θ_L (deg)	Absorber Ta (mg/cm^2)	Solid angle (msr)	Angle ϕ_L/θ_L (deg)	Absorber Ta (mg/cm^2)	Solid angle (msr)
30./90.	8.2	5.8	55./90.	8.2	5.8
45./90.	9.1	5.8	55./75.	8.4	5.8
55./90.	8.2	5.8	55./60.	8.6	5.8
60./90.	8.6	5.8	55./45.	9.1	5.8
70./90.	8.2	5.8	55./30.	8.2	5.8
75./90.	8.4	5.8			
85./90.	9.1	5.8			
100./90.	8.6	5.8			
115./90.	8.4	5.8			

similar heavy systems mentioned above the mass and charge distributions of the exit channel projectilelike fragment are well described by Gaussian distributions centered on the entrance channel values.[15,16] Even though the mass assumption employed is the most appropriate under the restriction that no charge or mass information is obtained directly from the experiment, it must be considered as a zeroth order approximation because the variances of the charge and mass distributions mentioned above can be quite large ($\sigma_Z^2 > 100$ for the largest energy losses).

In the course of these experiments the HI detectors (surface barrier, partially depleted, n-type Si) were exposed to approximately 10^8 particles/cm^2. This dose of very heavy ions produced significant damage in these Si detectors.[17] The radiation damage caused the pulse height to decrease with increasing dose. To correct for this pulse height loss, the slope of the energy calibration was increased as a function of dose. The change in the slope of the energy calibration from the beginning to the end of the experiment was $\sim 15\%$.

The detected energy of the heavy ion was corrected for pulse height defect following the prescription of Moulton *et al.*[14] The energies of all detected particles were corrected for the energy lost in the absorbers and the target using values of dE/dx calculated by the method of Rattazzi *et al.*[18] The stopping powers predicted by this formulation are within 10% of those given in the tables of Hubert *et al.*[19]

Since the fragment energies are measured after particle evaporation, their kinetic energies must be corrected for the energy lost in the evaporation process. The only significant correction to the DI fragment's mean kinetic energy due to evaporation arises from the lost mass. This correction was done by the iterative method described below. After the fragment energy is corrected to its expected value at the center of the target, the direction and energy of the undetected fragment are calculated with the mass assumptions described previously. The excitation energy (E^*) was calculated from the reaction Q value. This excitation energy was then divided between the two fragments in proportion to their masses, as suggested by the results of several studies.[1,4,5] The lost mass of the detected fragment (due to neutron emission) was taken to be $E^*/12$. The preevaporative mass was then used to recalculate the energy (using the same velocity), which was then used as the starting point of the next iteration. Two iterations were sufficient for the lost mass to converge within 1 u.

The Jacobian for the transformation of solid angles from the laboratory system into the rest frame of the targetlike fragment was calculated event by event. Subsequent sorting yielded energy spectra and angular distributions in the frame of the target recoil.

IV. ALPHA PARTICLE EMISSION SOURCE

The singles HI energy spectrum is shown in Fig. 1(a). At this angle (29°) there are strong elastic (EL) and quasielastic (QE) components that contribute to the peak above 1000 MeV. At lower energies the DI component is spread out over several hundred MeV. While the peak due to EL and QE scattering is dominant in singles mode, it is strongly suppressed when a coincidence between an α particle and the heavy ion is required, as shown in Fig. 1(b).

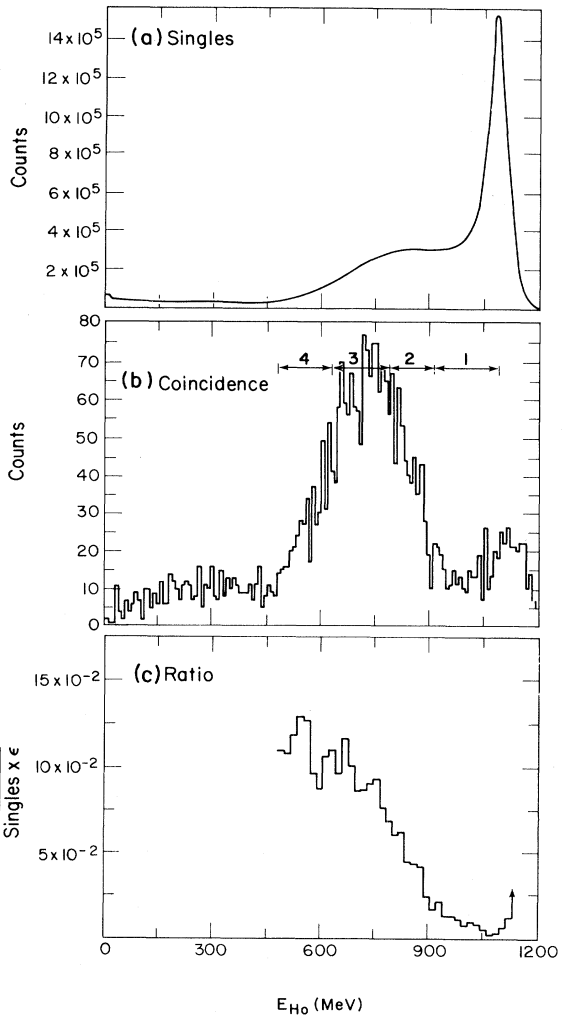

FIG. 1. (a) Singles energy spectrum of heavy ions detected at 29° (lab). (b) Energy spectrum of heavy ions detected at 29° in coincidence with an α particle detected on the opposite side of the beam at 55°. Four Q-value gates are indicated. Region 1 corresponds to the quasielastic region. The DI region is defined by the sum of regions 2, 3, and 4. (c) Ratio of coincidence [(b)] to singles yields [(a)] corrected for the coincidence efficiency. See text for discussion.

The ratio of coincidence yield (b) to the singles yield (a), corrected for the coincidence detection efficiency, is shown in Fig. 1(c). This figure indicates that the α-particle multiplicity is small in the EL and QE regions and increases as one moves across the DI peak to higher energy losses. This trend is expected due to the increasing temperature of the DI fragments as the energy loss increases. The multiplicity reaches a plateau at the low energy end of the DI component.

The laboratory energy spectra for α particles in coincidence with a heavy ion, with an energy in the DI region [the sum of gates 2, 3, and 4 in Fig. 1(b)], are shown in Figs. 2 and 3. The in-plane spectra (30° to 115° from the beam axis) and the out-of-plane spectra (0° to 60° out of the reaction plane, at an in-plane angle of 55°) are shown

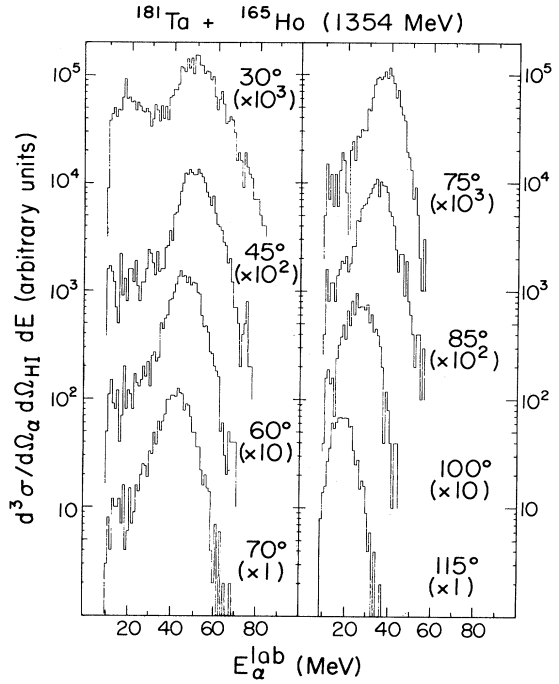

FIG. 2. In-plane laboratory α-particle energy spectra. In-plane laboratory angles are indicated.

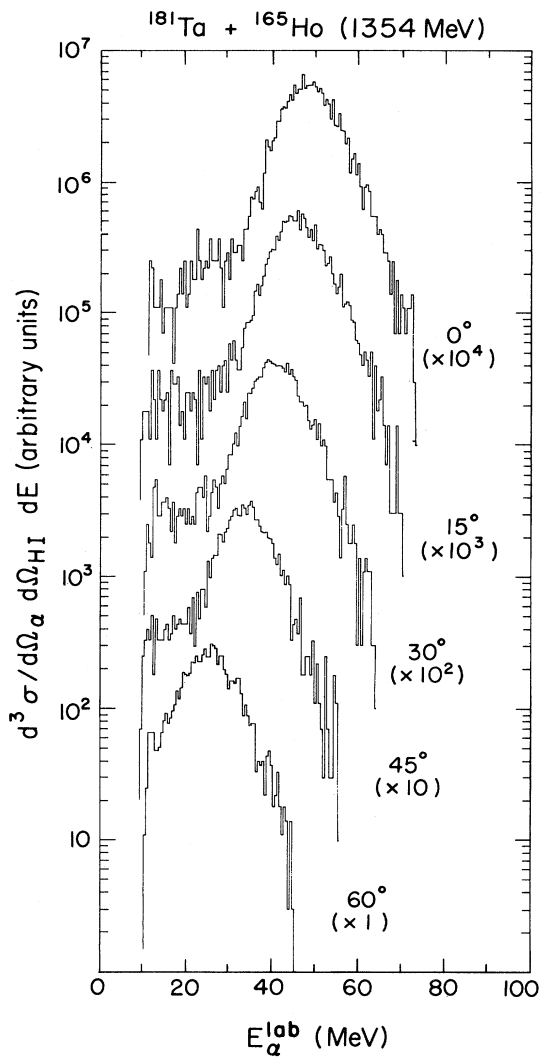

FIG. 3. Out-of-plane laboratory α-particle energy spectra. Out-of-plane laboratory angles are indicated.

in Figs. 2 and 3, respectively. The major features of these spectra can be summarized as follows. The in-plane spectra show that the peak energy for the two most forward angles is similar; however, as one proceeds to more backward angles the peak energy monotonically decreases with increasing angle. The out-of-plane spectra show a steady decrease in the peak energy as the out-of-plane angle is increased. An important feature in Fig. 2 is the presence of two separate peaks at the most forward angle (30°). These two peaks strongly suggest that there are at least two emission sources.

To determine these emission sources, the experimentally extracted root-mean-square velocity (v_α^{rms}) of the α particles is plotted in Fig. 4(a). Also shown are the velocity vectors for the detected projectilelike fragment (gated on the deep-inelastic events), the calculated velocity of the undetected fragment, and the velocity of the system center of mass. As this figure shows, the α-particle velocities are centered around the end of the velocity vector of the targetlike fragment. This demonstrates that the bulk of the α particles are emitted from the fully accelerated targetlike fragment. In addition, the low-energy component seen at 30° can be attributed to emission from the projectilelike fragment. This component is not seen at more backward angles because it drops below the detection threshold, which is shown by the dashed arc in Fig. 4(a).

Further evidence that the fully accelerated targetlike fragments are the source of emission can be obtained by examining the Q-value dependence of v_α^{rms}. In Fig. 4(b) the average velocity vector diagram for three different Q-value bins are plotted [corresponding to regions 2, 3, and 4 in Fig. 1(b)] along with the corresponding v_α^{rms}. A systematic motion for the locus of v_α^{rms} is seen that is explained by the change of the velocity of the targetlike fragment with Q value, as shown in Fig. 4(b). Owing to the heavy masses involved in this experiment, these velocity vector diagrams are relatively insensitive to the exact masses. For example, if one assumes that the mass of the detected fragment is 181 instead of 165 the change in the magnitude of the velocity vector is $<5\%$ (which is smaller than the change introduced by the Q-value binning procedure described above).

These vector diagrams indicate that the bulk of the α particles in the measured angular range are emitted from the targetlike fragment. However, a more sensitive indicator of the emission source can be obtained by examining the α-particle energy spectra in the rest frame of the targetlike fragment. If the strong component observed in the laboratory energy spectra is the result of evaporation from the target-recoil nucleus, then the α-particle spectra in the recoil frame should have the same spectral shape at all in-plane angles. These spectra are shown in Fig. 5 as a func-

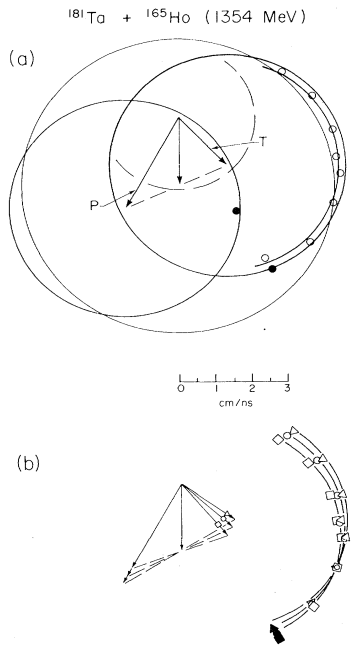

FIG. 4. (a) Velocity diagram. The letters P and T stand for projectilelike and targetlike, respectively. The open circles are the rms velocities extracted from the coincident laboratory α-particle energy spectra. The solid circles indicate the rms velocities of the two separate peaks that appear in the most forward angle data. The full large rings indicate the loci of expected α-particle velocities (Ref. 20) for the three different rest frames. For the targetlike fragment, the locus of velocities for a 10% reduction in the expected average emission energy is indicated by a partial ring. The detection threshold is shown as a dashed arc. (b) The velocity diagrams for Q bins 2–4 (all in the deep-inelastic region). The rms α-particle velocities for each bin are indicated. The smallest energy loss bin is indicated by triangles [bin 2 in Fig. 1(b)] and the largest energy loss bin by squares [bin 4 in Fig. 1(b)]. Three partial rings are drawn to guide the eye. They have the same radius and are centered on the three different recoil velocities.

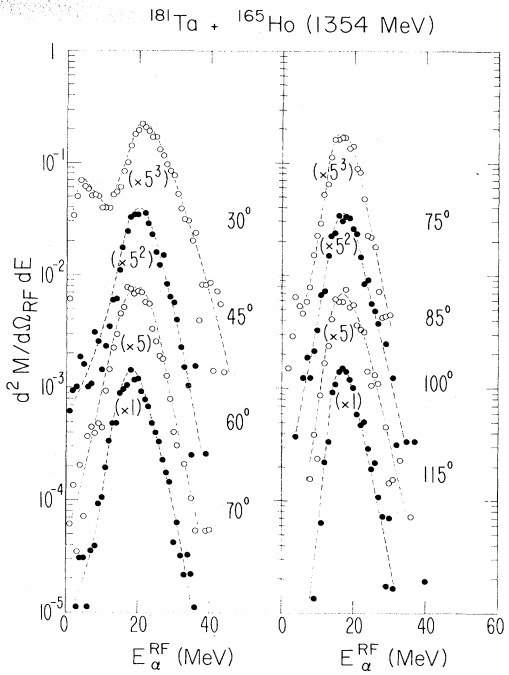

FIG. 5. The α-particle energy spectra in the rest frame of the targetlike fragment are shown. The dashed lines are drawn to guide the eye. The in-plane laboratory angles as measured from the beam axis are provided for reference. The double differential multiplicity is expressed in units of α particles $\times sr^{-1} \times MeV^{-1}$.

tion of in-plane angle in the laboratory. In the target-recoil rest frame the spectra are quite similar in shape and have peak energies of ~ 18 MeV, with the exception of the most forward angle data. While the spectra are quite uniform at backward angles, the most forward angle data show a somewhat higher average α-particle energy and an increased yield. This can be seen more clearly in Fig. 6 where the average α-particle energy for emissions from the targetlike fragment (the projectilelike emissions were removed by a low-energy threshold) and the differential multiplicity[21] are shown as a function of in-plane angle in the frame of the targetlike fragment. The targetlike fragment's recoil direction is arbitrarily taken as 0°. The isotropic yield and constant mean energy of the α particles show that the targetlike fragment is responsible for the bulk of emissions at angles equal to or larger than the recoil angle. However, there does seem to be an additional component that contributes at angles forward of the recoil direction causing both the differential multiplicity and the average α-particle energy to increase.

V. ANGULAR MOMENTUM AND THE OUT-OF-PLANE ANGULAR DISTRIBUTIONS

Since the bulk of the α particles emitted at angles near or behind the recoil angle are emitted from the target-recoil fragment, the out-of-plane angular distribution of α

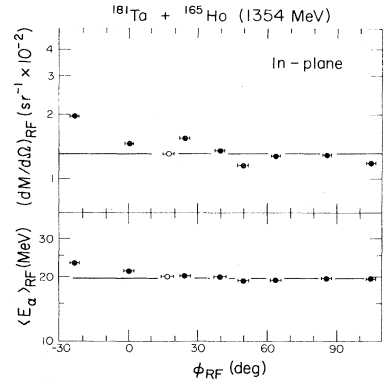

FIG. 6. (a) In-plane α-particle angular distribution in the rest frame of the targetlike fragment. The in-plane angle of $\phi_{RF}=0°$ corresponds to the recoil direction with negative angles towards the beam. The open circle is the in-plane point for the out-of-plane distribution. The horizontal error bars are estimates of the error in the angle between the target recoil fragment and the α particle due to the uncertainty in the primary mass of the detected heavy ion. (b) Average α-particle energies in the frame of the target recoil.

particles in this angular region contains information on the spin of the targetlike fragment. Out-of-plane data were acquired at an in-plane laboratory angle of 55°, which is close to but behind the average recoil angle (ϕ^L=47°). The measured α-particle energy spectra as a function of out-of-plane angle are shown in Fig. 7 (the in-plane angle is 55° for all the spectra). One should note that all these out-of-plane spectra are virtually identical in the rest frame of the targetlike recoil nucleus. The detector angle, as measured from the normal to the reaction plane, varies from 30° to 90°. The laboratory angle for the most out-of-plane spectra corresponds to approximately the normal to the reaction plane in the rest frame of the target recoil. Therefore, the entire 0°—90° range is covered by the data shown in Fig. 7.

The integrals of these spectra are shown in Fig. 8 as solid circles. This figure clearly indicates that there is a focusing of α particles into the reaction plane (90°). The ratio of the in-plane to out-of-plane yields is $\sim$1.4. This focusing is expected for an object spinning about an axis parallel to the normal to the reaction plane.

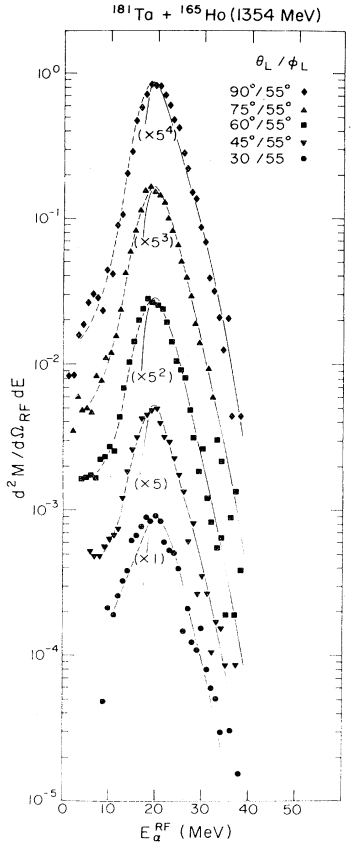

FIG. 7. Out-of-plane α-particle energy spectra in the rest frame of the targetlike fragment. The double differential multiplicity is expressed in units of α particles$\times$sr$^{-1}\times$MeV^{-1}. The key indicates the out-of-plane (θ_L) and in-plane (ϕ_L) laboratory angles as measured from the normal to the reaction plane and from the beam, respectively. The solid curves are the same for all spectra and are the result of an evaporation calculation (see text). The dashed lines are drawn to guide the eye.

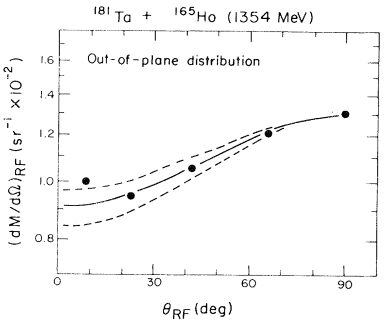

FIG. 8. The out-of-plane α-particle distribution. The emission angle is measured from the normal to the reaction plane. The size of the data points indicates the magnitude of the statistical errors. The solid line is a calculation, which is described in the text.

The transition state formalism developed by Moretto, Blau, and Pacheco[22,23] has been used to analyze the out-of-plane α-particle angular distributions. This method has been used previously in the analyses of both sequential fission[24,25] and α-particle[8] data. The choice of parameters for the analysis of the out-of-plane distribution from the ^{181}Ta + ^{165}Ho experiment is greatly simplified by a number of experimental observations. First, both α-particle emission and sequential fission are much less likely than neutron emission, therefore $\Gamma_n \approx \Gamma_T$. Furthermore, since the evaporation residue cross section is negligible, the minimum l wave (and thus $I_{\min}$, the minimum spin transferred from orbital to intrinsic fragment spin) is approximately 0. Under these conditions the angular distribution is predicted to be

$$\omega(\theta,\phi) \propto (1-e^{-I^2_{\max A}})/S(\theta,\phi)A \quad , \tag{1a}$$

where

$$A = \frac{\cos^2\theta}{2S^2(\theta,\phi)} - \beta \tag{1b}$$

and

$$S^2 = K_0^2 + \sigma_y^2 \cos^2\phi \sin^2\theta + \sigma_x^2 \sin^2\phi \sin^2\theta + \sigma_z^2 \cos^2\theta \quad . \tag{1c}$$

The parameter β accounts for the change in the relative α/n decay widths as a function of angular momentum. As is usual in fission theory, K_0^2 is the variance of the angular momentum projection on the separation axis. This variance can be related to the moments of inertia parallel ($\mathscr{I}_{||}$) and perpendicular ($\mathscr{I}_\perp$) to the separation axis,

$$K_0^2 = \frac{\mathscr{I}_{\text{eff}} T}{\hbar^2} = \frac{T}{\hbar^2}\left[\frac{1}{\mathscr{I}_{||}} - \frac{1}{\mathscr{I}_\perp}\right]^{-1} . \tag{2}$$

(See Ref. 23 for a detailed discussion of these parameters.)

For asymmetric systems there is both experimental[24–26] and theoretical[27,28] work that suggests that the variances σ_x^2, σ_y^2, and σ_z^2, are not equal. On the other hand, for near symmetric systems in-plane sequential fission angular distributions do not exhibit large anisotropies for DI events, indicating that the in-plane widths (σ_x and σ_z) are not sig-

nificantly different. This result supports the equilibrium model developed by Moretto and Schmitt[29] and Schmitt and Pacheco,[28] which predicts $\sigma_x^2 \sim \sigma_y^2 \sim \sigma_z^2$ for nearly symmetric systems. This model derives some additional support from its ability to reproduce the γ-ray anisotropies measured for similar systems.[13,30] Although γ-ray anisotropies are insensitive to the differences in the in-plane widths, and to first order insensitive to σ_z, they are sensitive to the misalignment (which is related to the magnitude of the in-plane spin component).

If the simplification suggested by the equilibrium model and supported by experimental data is employed, the parameter S is no longer a function of angle, i.e., $S^2 = K_0^2 + \sigma^2$, and the angular distribution reduces to

$$\omega(\theta') \propto (1 - e^{-I_{\max}^2 A})/SA \quad . \tag{3}$$

Although the experimental data do not suggest further simplifications in the form of the angular distribution, they do provide information on the remaining parameters. The ^{165}Ho + ^{165}Ho study[13] suggests values for both $I_{\max}$ and σ^2. Since the values of $I_{\max}$ are almost identical for the ^{165}Ho + ^{165}Ho and the ^{181}Ta + ^{165}Ho systems (the slightly larger interaction radius of the latter system is compensated by a lower average energy in the center of the target), the spin of an individual fragment deduced from the M_γ work can be used to estimate $I_{\max}$. For the ^{165}Ho + ^{165}Ho system the average primary spin per fragment is $\sim 33\hbar$ when one of the fragments is detected near the grazing angle. (See the center plot in the collage of plots in Fig. 9 of Ref. 13.) Since $I_{\max}$ in Eq. (3) is the maximum spin of a triangular distribution, it can be estimated from the average experimental spin,

$$I_{\max} = \tfrac{3}{2}\langle I \rangle \sim 50\hbar \quad . \tag{4}$$

The equilibrium model predicts that, for a symmetric system,

$$\sigma^2 \sim \mathcal{I} T \quad , \tag{5}$$

where $\mathcal{I}$ is the moment of inertia of one of the two fragments. In the present analysis the moment of inertia of a spherical fragment with the mass of the target was used ($\mathcal{I} \sim 83\hbar^2/\text{MeV}$). The temperature can be calculated from the average energy available for thermal excitation from

$$E^* = aT^2 \tag{6a}$$

with the level density parameter $a = A/8$ MeV^{-1} and

$$E^* = E_{\text{loss}} - E_{\text{rot}}. \tag{6b}$$

The small correction ($\lesssim 4\%$) for the energy involved in rotation of the fragments (E_{rot}) was calculated using rigid rotation predictions. The result is a temperature of 2.5 ± 0.1 MeV. Most of the error is due to the uncertainty in the detected fragment's mass.

The Q-value deduced temperature can be corroborated by the slope of the tail of the α-particle energy spectra. [Actually, the temperature deduced from the α-particle spectra should be slightly lower than the value deduced from the Q value due to the α-particle binding energy and the translational energy that are removed by the emission process. These energies, which should be subtracted from the right-hand side of Eq. (6), are much less than E_{loss} and change T by less than the uncertainty introduced by the mass uncertainty mentioned above.] The α-particle energy spectra also provide information on $\mathcal{I}_{\text{eff}}$. This is due to the fact that the critical decay shape for α-particle emission determines the relevant moments of inertia as well as the Coulomb barrier and thus the mean α-particle energies. Thus, by adjusting the critical decay shape so the α-particle energy spectra are reproduced $\mathcal{I}_{\text{eff}}$ can be calculated from the values of $\mathcal{I}_{||}$ and $\mathcal{I}_{\perp}$ for this configuration.

The α-particle energy spectrum was calculated using the formalism described in Ref. 22. To implement this formalism the critical decay shape was modeled by the equilibrium configuration of the rotating fragment plus α-particle complex in a spheroid-sphere model. Shape polarization and fluctuations about the equilibrium shape, which has a ratio of axes of ~ 1.1, were taken into account. The polarization and fluctuations contribute both to "sub-barrier" emission and to harder tails than would otherwise be present. The solid line superimposed on each of the five out-of-plane spectra shown in Fig. 7 was calculated by adjusting the surface separation ($s = 1$ fm) and radius parameter ($r_0 = 1.5$ fm). The close agreement between the data and the calculation (which uses a temperature of 2.5 MeV) in the region of the high-energy tail supports the Q-value deduced temperature. The calculation underpredicts the data in the low-energy region ($\lesssim 15$ MeV). This may be due to an inadequate shape parametrization of the critical decay shape or perhaps because the formalism does not explicitly include barrier penetration. Another possibility is that the very-low-energy portion of the spectra may be contaminated with some projectilelike emissions. This type of contamination would be most serious for the most out-of-plane spectrum because the average lab energy of the main component drops to only 15 MeV above the threshold, making it difficult to identify a still lower energy contaminant.

From the geometry and parameters for the critical decay shape given above, the values of $\mathcal{I}_{\perp}$ and $\mathcal{I}_{||}$ and thus $\mathcal{I}_{\text{eff}}$ were calculated. To calculate β (Ref. 23), the residual nucleus after neutron emission was taken to be spherical. Using these parameters, the out-of-plane distribution shown in Fig. 8 (solid line) was calculated using Eq. (3). The calculation agrees quite nicely with the data with the exception of the most out-of-plane point. The discrepancy between this data point and the curve is considerably larger than the statistical error (approximately the size of the points) and therefore must be attributed to a systematic effect.

The calculated shape of the α-particle out-of-plane angular distribution is quite sensitive to the parameters $I_{\max}$ and K_0^2 but is insensitive to the other parameters. The insensitivity to the magnitude of the misalignment can be seen by comparing the relative magnitudes of σ^2 and K_0^2. In this case $\sigma^2/K_0^2 \sim \frac{1}{7}$; thus the inclusion of σ^2 changes S^2 by only 14%. Since the shape of the angular distribution is roughly constant for a fixed value of $I_{\max}/S$, increasing I by $\sim 7\%$ compensates for the inclusion of σ^2. Because of this insensitivity, no effort was made to make further refinements concerning spin misalignments. Such refinements, which can include the effects of deformation and unequal misalignments, are important for sequential fission work where $\sigma^2 \sim K_0^2$.

The sensitivity of the calculation to the two most important parameters $I_{\max}$ and K_0 is illustrated in Fig. 8.

The dashed lines indicate a 10% change in either of the parameters. Explicitly, the upper dashed line is the result of a 10% decrease in I_{max} or approximately a 10% increase in K_0. Since these curves systematically disagree with the data, the average spin can be estimated to better than 10% if K_0^2 is well known.

VI. DISCUSSION AND SUMMARY

One conclusion from this study is that the bulk of the α particles detected at angles equal to or larger than the target recoil angle, in coincidence with a projectilelike fragment deflected into an angular region around the grazing angle, are emitted from the fully accelerated targetlike fragment. This result is consistent with most of the published light particle work for low-energy heavy systems.[1,2,4,5,8,31,32] However, several other studies[9–11] have found evidence for a large prescission component. In this latter work a bias towards the detection of LP's in coincidence with fusion-fission events was introduced by the detection of the HI at angles much larger than the grazing angle. On the other hand, in the present work (and most others[1,2,8]) a bias towards the detection of LP's in coincidence with DI events was introduced by the detection of the HI near or forward of the grazing angle. Since the lifetime of the compound nucleus is longer than that for the DI intermediate, one would expect a larger prescission component from the former.

The explanation of the difference in the experimental results appears to be more subtle than the one provided above. This is evident from the studies of α-particle emission in the $^{nat}Ag + {}^{56}Fe$ system at 480 MeV (Ref. 11) and of neutron emission in the $^{197}Au + {}^{63}Cu$ system at 365 MeV.[5] In the former case, most of the α particles detected in coincidence with a projectilelike fragment, detected near the grazing angle, were determined to be prescission. In the latter case, most of the neutrons detected in coincidence with a projectilelike fragment detected far behind the grazing angle were determined to be evaporated from the fully accelerated fragments. At the present time, the explanation of the different conclusions concerning the emission source of the bulk of the LP's is unclear. However, it should be mentioned that our data are not inconsistent with a small admixture of emissions from the center of mass system. Such emissions would be more forward focused and would have a larger average energy in the forward direction than emissions from the target recoil. Thus, a small admixture of evaporation from the composite system would perturb the forward angle data and provide an explanation for the increase in cross section and average energy we see at forward angles. However, the presence of a nonequilibrium component at forward angles (as suggested by the work of Refs. 9–11) could also be responsible for the observed deviations of our data at forward angles from a fragment emission model.

Although there are ambiguities concerning the emission sources of light particles, this study demonstrates that one can isolate a region dominated by fragment emission. Perhaps the most important result from the present study is that the general formalism described in Ref. 23 for the angular distribution of sequentially emitted particles, when coupled with input parameters extracted from the experimental data, does an admirable job of reproducing the out-of-plane α-particle distribution.

ACKNOWLEDGMENTS

We would like to thank the staff of the SuperHILAC for delivering a ^{165}Ho beam of sufficient intensity to enable us to do this coincidence experiment. This work was supported by the Director, Office of Energy Research, Division of Nuclear Physics of the Office of High Energy and Nuclear Physics of the U. S. Department of Energy under Contract DE-AC03-76SF00098.

*Present address: Department of Chemistry and National Superconducting Cyclotron Laboratory, Michigan State University, East Lansing, MI 48824.

†Present address: Comisión Nacional de Energía Atómica, Buenos Aires, Argentina.

[1]Y. Eyal, A. Gavron, I. Tserruya, Z. Fraenkel, Y. Eisen, S. Wald, R. Bass, G. R. Gould, G. Kreyling, R. Renfordt, K. Stelzer, R. Zitzmann, A. Gobbi, U. Lynen, H. Stelzer, I. Rode, and R. Bock, Phys. Rev. Lett. 41, 625 (1978).

[2]R. Babinet, B. Cauvin, J. Girard, J. M. Alexander, T. H. Chiang, J. Galin, B. Gatty, D. Guerreau, and X. Tarrago, Z. Phys. 295, 153 (1980).

[3]D. J. Morrissey and L. G. Moretto, Phys. Rev. C 23, 1835 (1981).

[4]D. Hilscher, J. R. Birkelund, A. D. Hoover, W. U. Schröder, W. W. Wilcke, J. R. Huizenga, A. C. Mignerey, K. L. Wolf, H. F. Breuer, and V. E. Viola, Jr., Phys. Rev. C 20, 576 (1979).

[5]J. Pèter, M. Berlanger, C. Ngô, B. Tamain, B. Lucas, C. Mazur, M. Ribrag, and C. Signarblieux, Z. Phys. A 283, 413 (1977).

[6]P. Glässel, R. S. Simon, R. M. Diamond, R. C. Jared, I. Y. Lee, L. G. Moretto, J. O. Newton, R. Schmitt, and F. S. Stephens, Phys. Rev. Lett. 38, 331 (1977).

[7]M. N. Namboodiri, J. B. Natowitz, P. Kasiraj, R. Eggers, L. Adler, P. Gonthier, C. Cerruti, and S. Simon, Phys. Rev. C 20, 982 (1979).

[8]L. G. Sobotka, C. C. Hsu, G. J. Wozniak, D. J. Morrissey, and L. G. Moretto, Nucl. Phys. A371, 510 (1981).

[9]D. Logan, M. Rajagopalan, M. S. Zisman, J. M. Alexander, M. Kaplan, and L. Kowalski, Phys. Rev. C 22, 104 (1980).

[10]D. Logan, H. Delagrange, M. F. Rivet, M. Rajagopalan, J. M. Alexander, M. Kaplan, M. S. Zisman, and E. Duek, Phys. Rev. C 22, 1080 (1980).

[11]D. Guerreau, D. Logan, M. S. Zisman, J. M. Alexander, E. Duek, and M. Kaplan, report, 1981 (unpublished).

[12]L. G. Sobotka, R. J. McDonald, G. J. Wozniak, D. J. Morrissey, A. J. Pacheco, and L. G. Moretto, Phys. Rev. C 25, 1693 (1982).

[13]R. J. McDonald, A. J. Pacheco, G. J. Wozniak, H. H. Bolotin, L. G. Moretto, C. Schück, S. Shih, R. M. Diamond, and F. S. Stephens, Nucl. Phys. A373, 54 (1982).

[14]J. B. Moulton, J. E. Stephenson, R. P. Schmitt, and G. J. Wozniak, Nucl. Instrum. Methods 157, 325 (1978).

[15]K. E. Rehm, H. Essel, P. Sperr, K. Hartel, P. Kienle, H. J. Körner, R. E. Segel, and W. Wagner, Nucl. Phys. A366, 477 (1981).

[16]W. U. Schröder and J. R. Huizenga, Annu. Rev. Nucl. Sci. 27, 465 (1977), and references therein.
[17]L. G. Sobotka, G. J. Wozniak, R. J. McDonald, and L. G. Moretto, Lawrence Berkeley Laboratory Report LBL-13366, 1981 (unpublished), p. 236.
[18]G. U. Rattazzi, R. P. Schmitt, G. J. Wozniak, and L. G. Moretto, Lawrence Berkeley Laboratory Report LBL-9711, 1980 (unpublished), p. 130.
[19]F. Hubert, A. Fleury, R. Bimbot, and D. Gardes, Institut de Physique Nucleaire Universite Paris-sud Report IPNO-RC-7807, 1978 (unpublished).
[20]M. F. Rivet, D. Logan, J. M. Alexander, E. Duek, M. S. Zisman, and M. Kaplan, report, 1981 (unpublished); J. M. Alexander, private communication.
[21]H. Ho, R. Albrecht, W. Dünnweber, G. Graw, S. G. Steadman, J. P. Wurm, D. Disdier, V. Rauch, and F. Scheibling, Z. Phys. A 283, 235 (1977).
[22]L. G. Moretto, Nucl. Phys. A247, 211 (1975).
[23]L. G. Moretto, S. K. Blau, and A. J. Pacheco, Nucl. Phys. A364, 125 (1981).
[24]D. J. Morrissey, G. J. Wozniak, L. G. Sobotka, A. J. Pacheco, R. J. McDonald, C. C. Hsu, and L. G. Moretto, Nucl. Phys. A389, 120 (1982).
[25]C. Le Brun, J. F. Lecolley, F. Lefebvres, M. L'Haridon, A. Osmont, J. P. Patry, J. Steckmeyer, and R. Chechik, Phys. Rev. C 25, 3212 (1982).
[26]P. Dyer, R. J. Puigh, R. Vandenbosch, T. D. Thomas, M. S. Zisman, and L. Nunnelley, Nucl. Phys. A322, 205 (1979).
[27]R. A. Broglia, G. Pollarolo, C. H. Dasso, and T. Døssing, Phys. Rev. Lett. 43, 1649 (1979).
[28]R. P. Schmitt and A. J. Pacheco, Nucl. Phys. A379, 313 (1982).
[29]L. G. Moretto and R. P. Schmitt, Phys. Rev. C 21, 204 (1980).
[30]A. J. Pacheco, G. J. Wozniak, R. J. McDonald, R. M. Diamond, C. C. Hsu, L. G. Moretto, D. J. Morrissey, L. G. Sobotka, and F. S. Stephens, Nucl. Phys. A397, 313 (1983).
[31]W. Kuhn, R. Albrecht, H. Damjantschitsch, H. Ho, R. M. Ronningen, J. Slemmer, J. P. Wurm, I. Rode, and F. Scheibling, Z. Phys. A 298, 95 (1980).
[32]I. Tserruya, A. Breskin, R. Chechik, Z. Fraenkel, S. Wald, N. Zwang, R. Bock, M. Dakowski, A. Gobbi, H. Sann, R. Bass, G. Kreyling, R. Renfordt, K. Stelzer, and U. Arlt, Phys. Rev. C 26, 2509 (1982).